공학석사학위논문

R-4bar-R 메커니즘
고관절 외골격 로봇의 생체역학적 평가

Biomechanical Assessment of
a Hip Exoskeleton Robot with R-4bar-R Mechanism

2023년 8월

서울대학교 대학원
기계공학부
김 태 환

R-4bar-R 메커니즘
고관절 외골격 로봇의 생체역학적 평가

Biomechanical Assessment of

a Hip Exoskeleton Robot with R-4bar-R Mechanism

지도교수 김 윤 영

이 논문을 공학석사 학위논문으로 제출함

2023년 4월

서울대학교 대학원

기계공학부

김 태 환

김태환의 공학석사 학위논문을 인준함

2023년 6월

위 원 장 : 윤 병 동 (인)

부위원장 : 김 윤 영 (인)

위 원 : 양 진 규 (인)

ABSTRACT

Biomechanical Assessment of a Hip Exoskeleton Robot with R-4bar-R Mechanism

Taehwan Kim
Department of Mechanical Engineering
The Graduate School
Seoul National University

This study evaluates the contribution of an exoskeleton robot equipped with a spherical revolute-4bar-revolute (R-4bar-R) mechanism to human walking through clinical trials and presents a path for improving exoskeleton robots using biomechanical information obtained from the trials. The exoskeleton robot employed in this study, through the application of the R-4bar-R mechanism to the hip joint, overcomes the limitations of traditional exoskeleton robots that are confined to assisting in single sagittal axis walking, by assisting in all three directions (flexion, abduction, and rotation) using a single actuator. Before the main clinical trial, simulation experiments were conducted using open-source data alongside several

preliminary clinical trials. From there, it was hypothesized that inclined walking would yield better results than level walking. And a target torque in the abduction direction, corresponding to 10% of the wearer's body weight, was established. We designed the clinical trial protocol to confirm This hypothesis for the biomechanical evaluation of the exoskeleton robot. Incorporating a ground reaction force meter, the protocol required the attachment of 24 infrared reflective markers to the lower limb. Subsequently, the subjects walked on a split-belt treadmill at a consistent speed of 1.25 m s^{-1}. The clinical trial consisted of three walking conditions (regular walking without a robot, assisted walking with a robot, and unassisted walking with a robot) performed for 5 minutes each on level ground and a 10% slope. Two healthy subjects were recruited for the trial, and data on the hip joint's angle and moment were collected and analyzed. The trial results indicated that the metabolic rate and joint moment were mainly elevated when the subjects walked with the assistance of the exoskeleton robot, whether on a level ground or an incline. The analysis of biomechanical results revealed various causes for the discrepancies between the observed results and the intended design of the mechanism. To achieve practical auxiliary effects, this study suggested first that the alignment of the R-4bar-R mechanism and the thigh (the end effector) was parallel. Secondly, we propose adjusting the target torque to match the three-directional moment required by the human body synchronously, rather than limiting the target torque to a singular abduction moment, and employ an automatic control model utilizing a Human-in-the-Loop approach. We have, lastly, suggested the need for weight reduction by

changing the material and modifying the design of the flexible shaft connection part. I expect that the effectiveness and suggested improvements of the hip joint assist exoskeleton robot with the spherical R-4bar-R structure proposed in this study will make a significant contribution to overcoming the limitations of single-joint exoskeleton robot research and will help in the expansion of multi-axis joint exoskeleton robot research.

Keywords: Biomechanics, Kinetics, Metabolic, Exoskeleton Robot, Wearable Robotics, Gait Analysis

Student Number: 2021-21839

CONTENTS

LIST OF TABLES

LIST OF FIGURES

CHAPTER 1.
INTRODUCTION

Lower limb exoskeleton robots are gait aid devices designed to fit the wearer's body and programmed with control algorithms that compensate for lower extremity movements at the precise gait phases [1–3]. They can reduce the energy cost by pushing or pulling body segments with motors to assist with walking or movement in daily living activities [4, 5]. Various types of exoskeleton robots depend on the joint the robot assists. Some lower limb exoskeleton robots assist all joints (hip-knee-ankle) to save energy consumption [6, 7]. Several exoskeleton robots simultaneously support the hip and ankle joints [8] or knee and ankle joints [9]. Patrick W. [10] demonstrated that a whole-leg assistance exoskeleton robot could significantly improve metabolic cost relative to walking with one and two-joint support exoskeleton robots. However, many exoskeleton robots were designed to assist only the hip or ankle joints because they were smaller, lighter, cost-effective, and easier to control than two or three joints [10, 11]. Some lower limb exoskeleton robots support all joints (hip-knee-ankle) to reduce energy consumption [6, 7], specifically hip and ankle joints [8] or knee and ankle joints [9] simultaneously. Patrick W. [10] demonstrated that a full-leg assisted exoskeleton robot can significantly improve metabolic costs compared to walking with one- and two-joint-supported exoskeleton robots. But, most of these exoskeleton robots have limitations in assisting movement only in the sagittal plane. Numerous studies have an experiment to reduce energy consumption or restore ambulation ability lost from disability [12]. Because movements of humans, especially gait, tend to select gait parameters to minimize energetic cost [13–15]. In this respect, the hip joint exoskeleton robot has received much attention over many years due to its biomechanical properties, which offer crucial metabolic improvement [16, 17].

Many studies in recent years show exoskeleton robots have reduced metabolic costs by assisting one or two joints [1, 11, 18, 19]. For example, it has many possible uses in the rehabilitation field through learning to gait with the proper trajectory required for walking [20]. It also has been investigated as potentially increasing productivity in the manufacturing industry and military personnel by improving mobility [7, 21]. These exoskeleton robots are mainly designed with a single joint to assist the movement of walking and have a single axis the flexion and extension. Therefore, many studies have been confined to the biomechanical analysis of these sagittal assistance motion effects [4, 22, 23]. However, Since the human hip joint anatomically forms a ball-shaped femur head located in the concave pelvis socket, it does not move in only a single plane during walking but moves on a spherical plane according to the gait phase [24–26]. Therefore, to effectively support the diversity of hip joint movements, the joints of the exoskeleton robot also have a position similar to the hip joint rotation axis, and the leg movements must be assisted with complex moments in two or more directions [27]. When one-foot swings, the pelvis on the same side tilts downward to prevent the toe from dragging on the floor, the pelvis must be kept level with the ground. This action is achieved by the contraction of the gluteus medius muscle on the weight-supporting side, causing abduction. This action is a form of closed kinetic chain exercise and results in significant energy consumption in the human body, so it is necessary to assist the abduction movement in the exoskeleton robot. To solve the human-exoskeleton interaction challenge, Kang et al. [28] suggested a hip joint link apparatus called the R-4bar-R system that can assist all three-dimensional movements of the hip joint with a single actuator.

The exoskeleton robot we developed applied a spherical 4-bar linkage system with three degrees of freedom to the hip joint to create a complex moment with a single mechanism, which has the advantage of creating a three-dimensional movement with one actuator. Considering the anatomical movement of the hip joint during walking, the hip joint of the supporting foot is stepping forward and weight support in the vertical direction through maximum flexion and extension motions in 0-40% of the gait phase. At this time, rotational monement of the hip joint is accompanied to pull forward the opposite pelvis. Afterward, the hip joint is extended up to 60% of the gait phase, the weight is shifted forward, and the hip joint is externally rotated to move the opposite pelvis forward [29, 30]. To support the pelvis so that the swinging leg does not drag on the floor during the 0-60% gait phase, the abduction moment to support body weight is maintained at the highest level, deriving the most significant energy consumption during walking [31]. We focused on that keeping the pelvis on a horizontal level takes a lot of energy during the stance phase. Playing agonistic muscle for this movement, the gluteus medius is substantial fan-shaped muscle located in the posterior hip, stretching from the ilium to the proximal femur. We developed a spherical mechanism called the R-4bar-R system that can assist all three-dimensional movements of the hip joint with a single actuator to reduce energy cost by mainly supporting this muscle and assisting the movement of the hip joint in the frontal and horizontal plane.

In this study, we have meaningful comparative assessments to verify the characteristics of this new system through clinical trials of level walking and inclined walking on a treadmill. Our study involved simulating an assistance moment trajectory aimed at reducing the measured metabolic cost of walking, and we compared this scenario to walking without any assistance of exoskeleton robot. We measured biomechanical parameter changes in the respiratory quotient to verify how the exoskeleton we designed assisted and affected the potential biomechanical kinetics contributing to metabolic improvement. The protocol entailed walking on level ground and on an incline under three different conditions (normal walking without an exoskeleton robot, walking with assistance, and without assistance while wearing an exoskeleton robot) on a treadmill at a constant speed. Using this protocol, we measured the pure metabolic rate and the angle and moment of the hip joint to assess how the R-4bar-R exoskeleton robot we designed could improve biomechanical parameters.

(a)

(b)

(c)

Fig. 1.1 Experimental environment and exoskeleton robot with R-4bar-R mechanism. (a) Front view, (b) side view, (c) rear view.

CHAPTER 2.
METHOD

2.1 R-4bar-R exoskeleton system

The spherical R-4bar-R linkage system suggested by Kang [28] is the three-DOF hip joint mechanism that consists of two revolute joints and one four-bar mechanism connected in series. Unlike the single-joint hip joint mounted on conventional exoskeleton robots, this mechanism can deliver the triaxial moment like the human anatomical hip joint by a single actuator. As shown in Fig. 2.1, an exoskeleton robot with an R-4bar-R mechanism is designed to simultaneously transmit the assistance torques to the hip joint in three ways (flexion/extension, abduction/additional, internal and external rotation). When the input torque and the angle of the 4-bar linkage mechanism are determined, the magnitude and direction of the moment at the end effector are determined. Three axial motions of this mechanism can calculate and further assist the movement of the diversifying human body joint axes in the 3D space. We designed an exoskeleton robot using these characteristics of the R-4bar-R mechanism, and it was thought that it would contribute to reducing energy consumption during walking by helping the movement of the hip joint in all directions by mainly assisting the abduction moment and assisting the flexion and rotation moment at the same time.

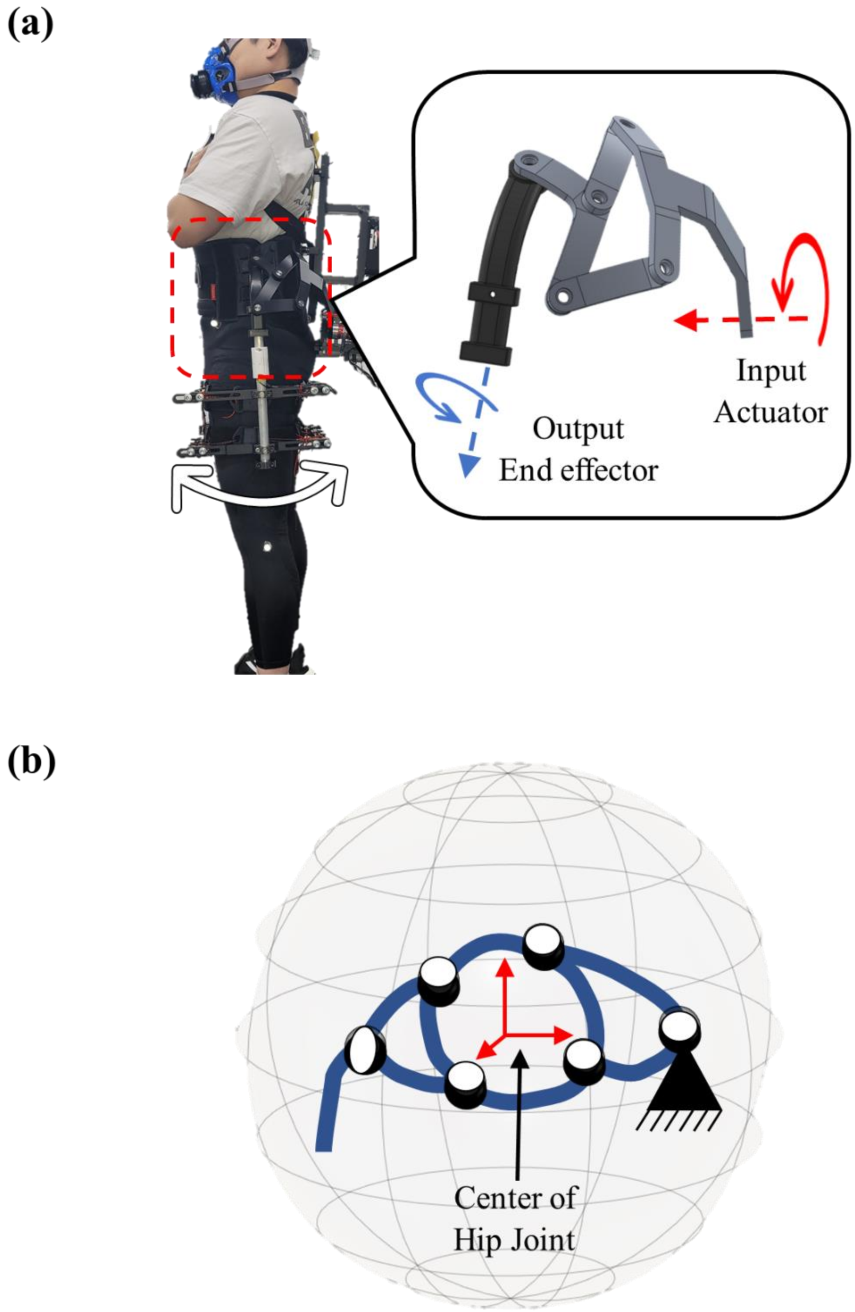

Fig. 2.1 Spherical R-4bar-R mechanism. (a) R-4bar-R exoskeleton robot and force transmission system from the flexible shaft. (b) Topology of R-4bar-R mechanism.

Triaxial hip joint output moments were simulated using open-source data from 50 subjects to predict clinical outcomes. Based on this data, it was requested to output 90% of the abduction moment during level and inclined walking. We analyzed the flexion and rotational moments created by the R-4bar-R mechanism according to the outputted abduction moment. The average moment of 50 people using the open source was normalized by body weight and normalized to a 100% gait cycle from heel contact to the next heel contact. When the results are analyzed for the design of the clinical trial protocol, the green box (10~40% gait cycle range) in Fig. 2.2 (a) shows that when an input torque of 90% of the body weight is applied, a flexion component that interferes with the red extension moment required by the human body is observed in incipient 40% of the gait cycle.

On the other hand, looking at the blue box in Fig. 2.2(b), the R-4bar-R mechanism system properly transfers three-way moments to the human body during the entire gait except for the short section (40~43%) of the gait cycle under the inclined walking condition. Excluding the abduction moment, a comparison of the gait cycle sections in which the exoskeleton robot assists human body movement shows 46.7% of the flexion assistance section and 40.0% of rotation assistance during level walking, and 52.0% of the flexion assistance section and rotation assistance during inclined walking is 45.3%. Based on these results, it was predicted that the robot used in this study would have beneficial results in reducing the energy consumption of the human body when walking on an incline compared to walking on level ground, and a clinical trial protocol was designed to verify this hypothesis.

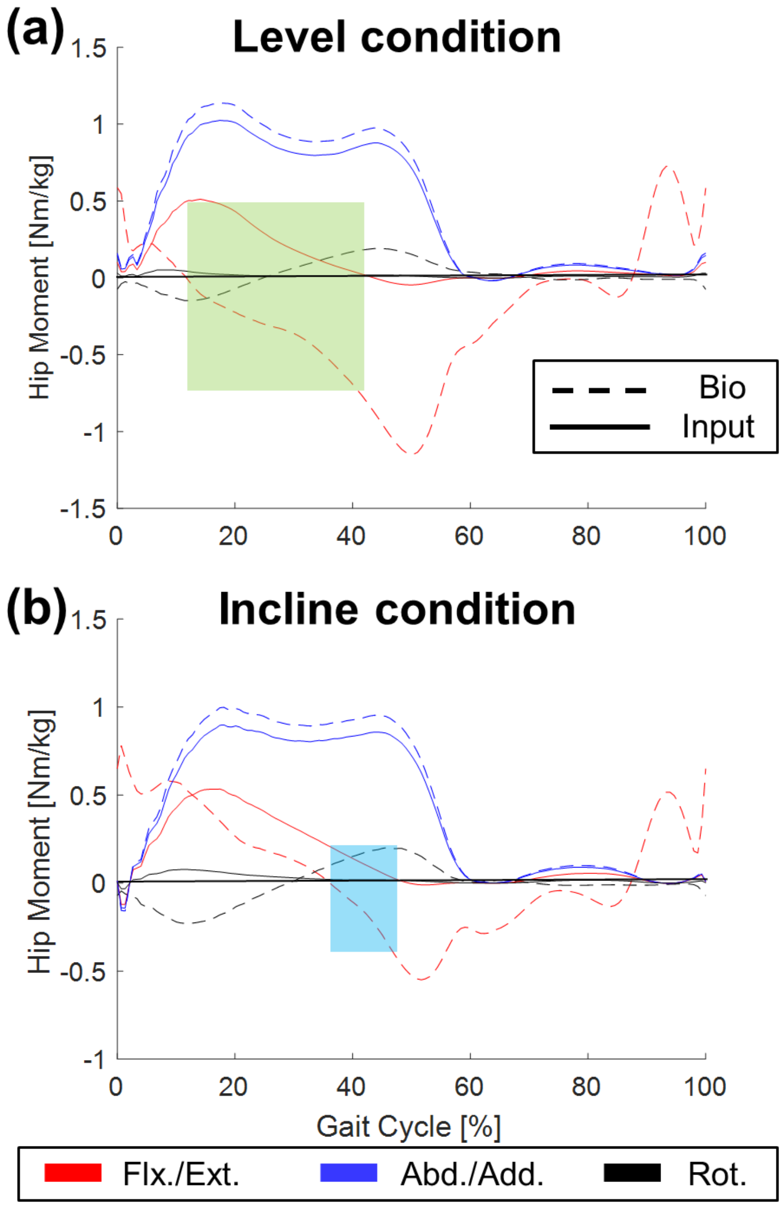

Fig. 2.2 Input moment according to the abduction moment. Reference biological moment is calculated when the standard abduction moment is 90% of the body weight in time. The dotted line is the moment the human body requires during walking, and the solid line is the output moment from the exoskeleton robot. (a) level walking condition. (b) 10% incline condition.

2.2 Participants information

A local convenience sample comprised two healthy male volunteers, aged 23.5 years, with an average height of 172.5 cm and an average mass of 76.0 kg. The participants willingly took part in the study following the provision of informed consent. Furthermore, in order to mitigate the impact of adaptation, we specifically selected two participants with no prior experience using an exoskeleton robot. All participants noticed the precise information about the test process and the risks before participating and provided written consent.

The following criteria were used for participant inclusion: 1) Healthy adult males/females over 19 years without physical or mental disabilities. 2) Those who had not experienced orthopedic injuries that may affect walking in the past three years. 3) People who could walk more than 10m without assistive devices. 4) Those who did not have cognitive impairment could communicate and faithfully participate in the research process. 5) People who signed an agreement document after hearing about the experimental method.

Participant exclusion criteria were as follows: 1) Individuals with psychiatric disorders. 2) Those who exhibited pathological gait during 10-meter walking. 3) People with cardiovascular and musculoskeletal diseases. 4) Minors or adults over 60 years old. 5) Those deemed inappropriate by the researcher.

The institutional review board (IRB) of Seoul National University (IRB No. 2209/004-008) approved the study design and protocol. None of the participants had prior experience in walking with an exoskeleton robot.

2.3 Experimental protocol design

The present study investigates the locomotor performance of untrained individuals utilizing an exoskeleton robot for gait assistance on a split-belt treadmill installed force plate. The clinical trial environment can be seen in Fig. 2.2. The study examines their gait ability at a consistent velocity of 1.25 m s^{-1} across two distinct surface inclinations, 0% and 10% surface gradient (equivalent to 0 degree and 5.7-degree inclination angle), under unpowered and powered conditions. To mitigate potential adaptation effects, the implemented protocol was thoughtfully designed as a single-day protocol without any training sessions. In addition, participants have another walking trial without the exoskeleton robot to compare the two conditions of walking with the exoskeleton on. To minimize the effect of fatigue and test conditions during the walking with exoskeleton test, two different exoskeleton conditions (unassisted walking and assisted walking with an exoskeleton robot) were conducted in randomized order, and to minimize the fatigue caused by the device's weight and external power transmission, normal walking without an exoskeleton robot was performed as the last step.

The input torque from the motor was determined as 10% of the body weight through a pilot test before conducting the main experiment with single-participant. In the pilot test, the generator applied 10% and 15% torque and respiratory gas under the same condition as the primary test at a steady speed of 1.25 m s^{-1} and two different inclination surfaces (0%, 10% surface gradient). As shown in Fig. 2.3 (a) and (b), Since the metabolic rates at the 15% input torque condition were higher than that of

10% input torque in both slope conditions, it was determined that 10% input torque was more appropriate for the exoskeleton robot used in this test. Metabolic rate results in 10% incline walking results tend to be higher than the leveled surface walking results because the pilot test was also a single-day test, and the participants' fatigue was accumulated by performing eight different test conditions while wearing a mask for respiratory gas measurement. As evidenced in Fig. 2.4 (a), the clinical test protocol was devised with the objective of mitigating fatigue resulting from cumulative walking time. To achieve this, the test order for the two subjects was alternately arranged, allowing each subject to have sufficient rest periods during the test. This strategic design aimed to minimize the impact of fatigue and optimize the test conditions, thereby enhancing the reliability of the experimental findings.

Based on the pilot test results, the study recognized that prolonged wearing of the breathing gas mask and the exoskeleton robot impairs respiration, thereby significantly impacting the test outcomes. Consequently, the test protocol was meticulously designed to prioritize reducing wearing time for the robot, breathing gas mask, and exoskeleton robot, aiming to mitigate the effects mentioned earlier and optimize the validity of the experimental findings. To enhance the reliability of the results and alleviate fatigue, the first subject performed the test in the order of level and slope, while the second subject performed the test in the order of slope and level, with alternating breaks between the subjects during the clinical test. The reflective markers were meticulously positioned in the initial session on the test subjects. Additionally, the alignment of the harness, crucial for integrating the robot with the human body, was carefully verified. Following this, the test subjects wore a respiratory gas measurement mask and were instructed to stand stationary for 5 minutes to determine their basal metabolic rate. Lastly, the robot was donned using a specially designed harness, completing the preparatory measures before initiating the walking test. In the second session, powered and unpowered conditions were randomized after donning the robot, with a 5-min break between the two walking conditions, to minimize the effect of the order on the results. Finally, after removing the robot, we performed a normal walking test. All three walking conditions performed in the second session were standardized, each lasting 5 minutes. At the end of the walking test, two subjects completed a written questionnaire about how they felt while wearing the robot exoskeleton and completed all clinical trial protocols.

(a)

(b)

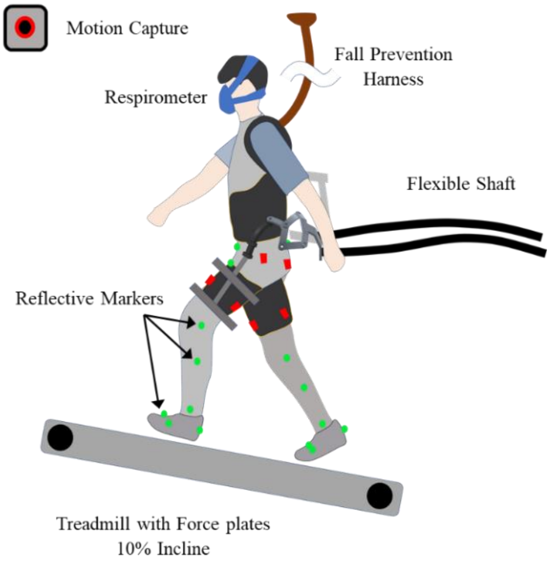

Fig. 2.3 Experimental condition. (a) participant performed their walking tasks with a split-belt treadmill installed force plates with constat speed. Walking speed is 1.25 m s^{-1} in two inclination conditions(0% level, 10% incline). (b) The infrared camera system tracked the reflective markers(green).

(a)

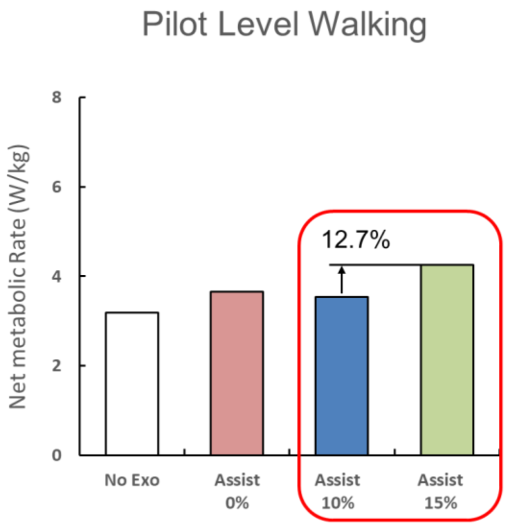

(b)

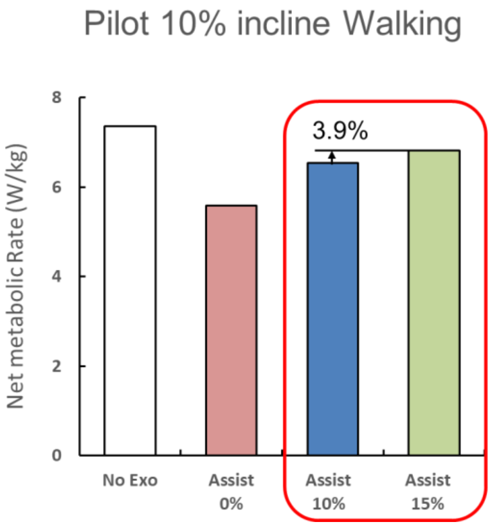

Fig. 2.4 The net metabolic rates were determined for each slope condition and were computed by subtracting the standing still state from the average value measured during the final 2 minutes, subsequently normalized to body weight. (a) level walking in constant speed. The net metabolic rate exhibited a 12.7% reduction when using a 10% assist compared to a 15% assist condition. (b) 10% uphill condition walking. The net metabolic rate demonstrated a 3.9% decrease when utilizing a 10% assist compared to a 15% assist condition.

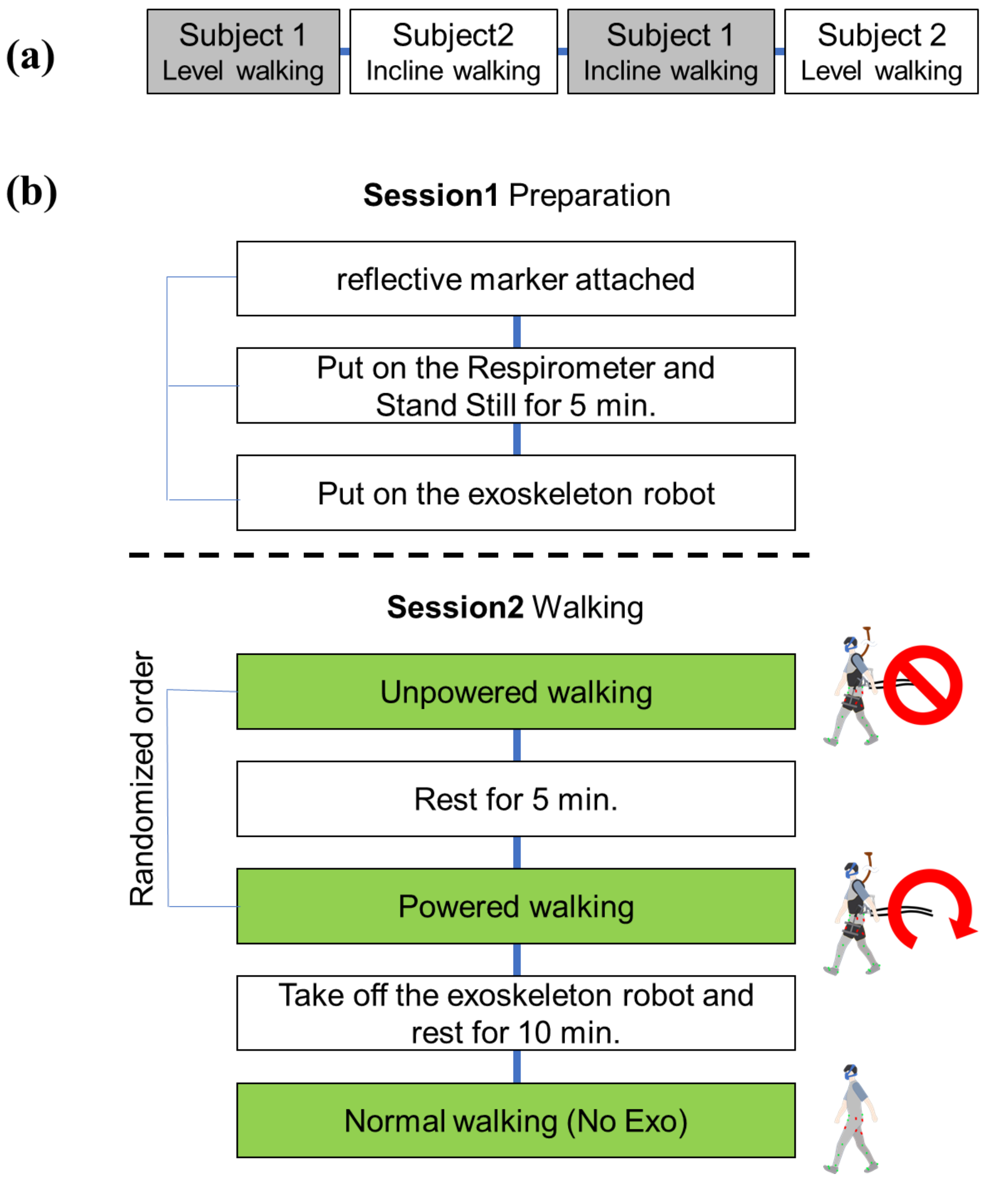

Fig. 2.5 The experimental protocol. (a) Treadmill inclination conditions and test sequence according to subjects. (b) The experiment was conducted randomly to minimize measurement errors, such as fatigue accumulation based on the walking sequence. In the final sequence, the participants performed normal walking without wearing the robot. A minimum rest period of 5 minutes was granted between walks, and an additional 5-minute break was offered upon request by the subjects.

2.4 Data collection and specialized equipment for the study

As shown in Fig. 2.3 (b), subjects wore a breath mask connected to a gas analysis system that measured O2 consumption and CO2 production (K5, Cosmed, Rome, Italy). For each trial, respiratory data were collected during the last two minutes. All lower limb 3-axial agles were collecteded with 24 reflective markers (two on the anterior superior iliac spine, two on posterior superior iliac spine, four on each foot, two on each knee joint, on each shank and thigh for tracking) using 8 motion capture cameras (250 Hz; MX10, Vicon, Oxford, UK) with Vicon software, and The three-dimensional ground reaction forces (GRFs) were captured using an instrumented treadmill (1000 Hz; Bertec, Columbus, OH, USA). Kinematic and kinetic data were averaged for two strides of each condition, which included a 5-minute trial.

2.5 Data analysis method

The Brockway formula [32] was utilized to calculate the metabolic data from which the resting metabolic cost was subtracted in the walking conditions to derive net metabolic data. These values were futther normalized by body weight to obtain the net metabolic rate [18]. Kinematics and kinetics acquired data were filtered with a Butterworth low-pass filter (cutoff frequency of 6Hz) to filter the sensor noise for analyzing the lower limb movement. The raw data we acquired were processed with Visual 3D (C-Motion, MD, USA). To ensure consistency, right hip angles and moment data for the right leg were time-normalized from right heel contact to the subsequent right heel contact, with the moment values further normalized by body weight.

CHAPTER 3.
Experimental Result

3.1 Net metabolic rate

In the first session, as depicted in Fig. 3.1 (a), Subject 1 engaged in level ground walking, providing an opportunity to observe net metabolic rate. From left to right, subject 1 demonstrated a net metabolic rate of 3.07 W kg^{-1} without the aid of the exoskeleton robot. When the subject donned the exoskeleton robot and walked without robotic power, a notable increase of 34.7% in metabolic rate was observed, reaching 4.14 W kg^{-1} compared to the baseline rate without the robot. The metabolic rate further escalated to 4.41 W kg^{-1}, marking a 43.6% increase compared to walking without the exoskeleton robot when first subject employed the robot for walking assistance. These observations indicate that first subject expended the highest amount of pure metabolic energy when wearing the exoskeleton robot and utilizing its assistance for level-ground walking.

Subject 1 performed walking exercises on a treadmill set at a 10% incline during the second session. The walking trials commenced with the subject wearing the exoskeleton robot but walking without its assistance. This sequence was followed by the subject wearing the exoskeleton robot and walking with its assistance, and finally, the subject engaged in normal walking without the exoskeleton robot. As represented in Fig. 3.1 (b), the recorded metabolic rates are as follows: 8.38 W kg^{-1} for normal walking (from the left), 7.45 W kg^{-1} for unassisted walking post-donning of the exoskeleton robot, and 7.09 W kg^{-1} for walking with the aid of the robot. This incline walking session revealed a generally elevated metabolic rate compared to level ground walking. While Subject 1 took a break for one and a half an hour during the testing period of Subject 2, the highest pure metabolic rate was still observed during the final normal (without EXO) walking trial. Nevertheless, due to fully adapting to the exoskeleton robot during level walking, the subject experienced a 3.2% decrease in metabolic rate when walking with the robot's assistance, compared to unassisted walking.

To minimize the influence of test order, Subject 2 initially walked on a treadmill set at a 10% incline during the first session, followed by level ground walking in the subsequent session. Fig. 3.2 illustrates this, with panel (a) representing level ground conditions and panel (b) depicting incline conditions. Under the level ground condition, the sequence of trials was as follows: first, the subject wore the exoskeleton robot but walked without assistance; second, the subject wore the exoskeleton robot and walked with its assistance; finally, the subject performed normal walking without wearing the robot. As shown in Fig. 3.2 (a), the net metabolic rate of Subject 2 under level ground conditions was 4.20 W kg^{-1} when walking normally without wearing the exoskeleton robot (from the left). Upon wearing the exoskeleton robot without assistance, a considerable decrease of 43.9%

was observed, resulting in a rate of 2.35 W kg^{-1} compared to normal walking. Finally, when walking with the assistance of the robot, a significantly higher metabolic rate of 5.69 W kg^{-1} was recorded, indicating a 35.7% increase compared to the normal walking condition.

Figure 3.2 (b) illustrates the net metabolic outcomes from the 10% incline walking trial of Subject 2 during the first session. Like Subject 1, the metabolic rate peaked at 7.68 W kg^{-1} during normal walking without the robot. When wearing the robot without assistance, the net metabolic rate of subject 2 declined to 5.40 W kg^{-1}, marking a 29.7% decrease from the normal walking condition. In the case of robot assistance, the net metabolic rate further decreased to 5.99 W kg^{-1}, a reduction of 21.9%. Notably, despite the first session involving a 10% incline walk on the treadmill, the net metabolic rate was the highest during the level ground walking condition with robot assistance due to the initial lack of robot adaptation. Notably, irrespective of the test sequence, both subjects exhibited the highest net metabolic rate during normal walking without the robot on an incline. Furthermore, the net metabolic rate appeared to be at its peak when level ground walking was undertaken with the assistance of the exoskeleton robot.

Sub1

(a) (b)

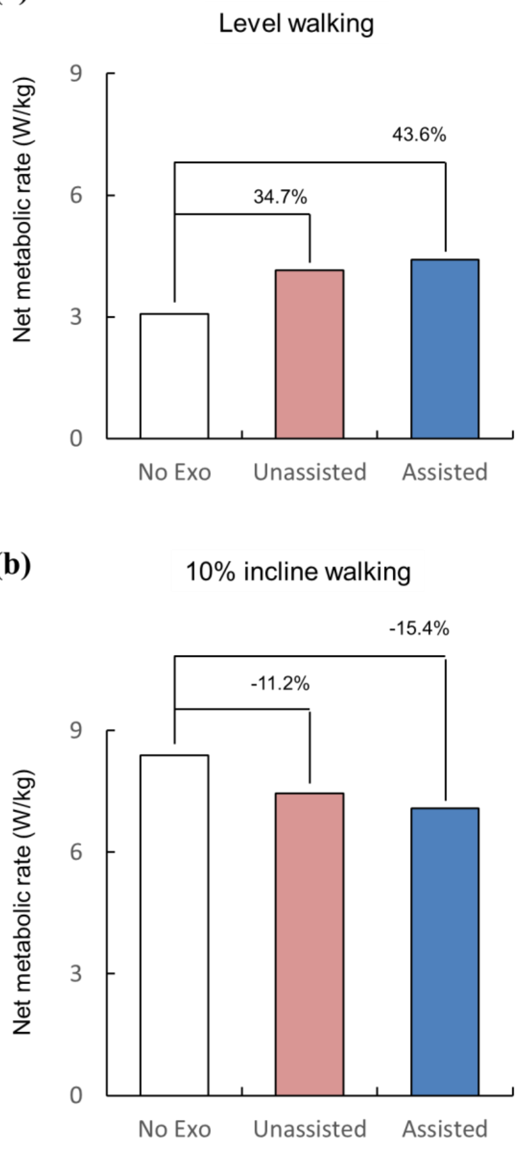

Fig. 3.1 Metabolic rate of first subject. (a) In the level walking condition, the assisted condition showed a 43.6% higher result than the no exo condition. (b) In the 10% inclined walking condition, the assisted condition resulted in a 15.4% lower result than the no exo condition.

Sub2

(a)

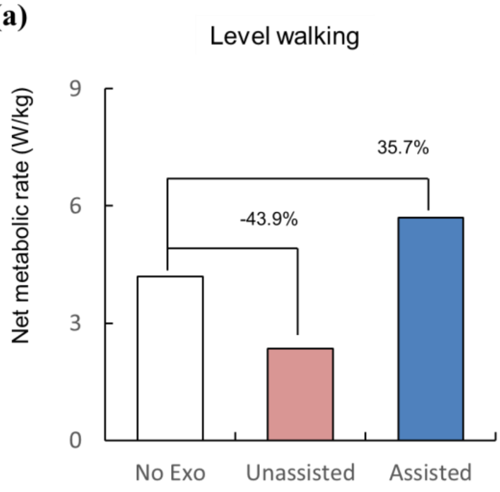

(b)

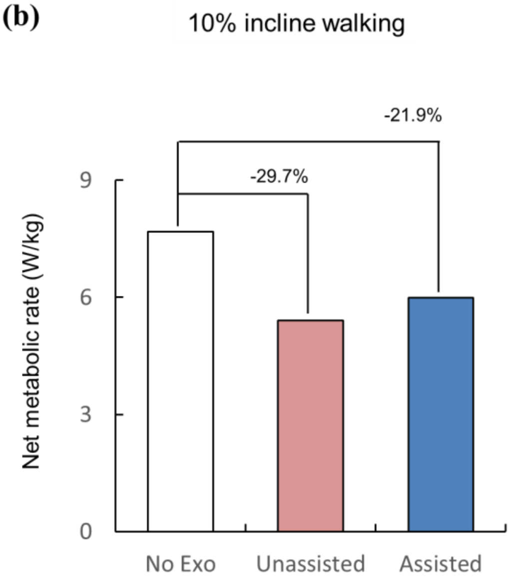

Fig. 3.2 Metabolic rate of second subject. (a) In the level walking condition, the assisted condition showed a 35.7% higher result than the no exo condition. (b) In the 10% inclined walking condition, the assisted condition resulted in a 21.9% lower result than the no exo condition. In both conditions, the unassisted condition resulted in the lowest net metabolic rate.

3.2 Kinematic analysis of hip joint motion

This study aims to evaluate the effects of the flexion moment and rotation moment on the gait of the wearer of the R-4bar-R Exo robot when an abduction moment, corresponding to 10% of the wearer's body weight, is given as the target torque. To achieve this, we recruited two healthy subjects, attached 24 reflective markers to their lower limb segments, and analyzed the hip joint angle on level and inclined walking. Each kinematics Figure displays the hip joint angle results during level walking and 10% incline walking under three conditions: no exoskeleton (no exo), unassisted with an exoskeleton robot, and assisted from an exoskeleton robot. For these results, we defined a single stride, considered 100% of one cycle, as the cycle starts with the right heel strike and ends when the same right foot touches the ground again.

Figure 3.3 presents the angle of the hip joint during level walking of the first subject. When the exoskeleton robot-assisted in walking, the hip joint displayed a flexion angle that was 10 degrees less compared to the 'no exo' condition. However, the hip joint extended 10 degrees more during propulsion after 30% of the walking phase (mid-stance). The middle graph representing adduction/abduction direction shows that although the robot received an abduction moment during the stance phase, the hip joints were adducted more than 5 degrees compared to the 'no exo' condition, indicating an abnormal gait. Inspecting the final rotation graph, it can be seen that compared to the 'no exo' condition, both external and internal rotation of the hip joint exhibited repeated movements when the exoskeleton robot-assisted.

Figure 3.4 presents the results of the changes in the angle of the hip joint during the first subject's inclined walking. When the robot assisted in walking, compared to the 'no exo' condition, the hip joint exhibited greater flexion, did not fully extend from the initial weight-bearing phase to the propulsion phase, and demonstrated increased flexion during the swing phase. Reviewing the graph representing the adduction/abduction direction, there can be observed that an abnormal gait with about 5 degrees more adduction occurred when assisted by the robot, similar to level walking, and more abduction was noted during the swing phase. Upon analyzing the final rotation graph, it was confirmed that external and internal rotation were repeated when the exoskeleton robot assisted, as observed in the level ground condition. Still, the range of change was less than that in level ground walking.

Figure 3.5 presents the angle of the hip joint when the second subject walked on level ground. Comparing the movements in the sagittal plane of the hip joint when the robot assists with walking to the 'no exo' condition, more flexion during the weight-bearing phase and more extension during the propulsion phase can be observed. Reviewing the middle graph illustrating the adduction/abduction direction, it can be seen that, similar to the first subject, the adduction movement is more prominent when the robot assists with walking. Still, the angle difference is not substantial, and the overall trend is similar. Upon analyzing the final rotation graph, a fluctuation of more than 10 degrees was observed in the initial weight-bearing phase when assistance was provided by the robot, compared to the 'no exo' condition. However, the movement was similar to the hip joint angle of the second subject.

Figure 3.6 presents the results of the changes in the hip joint angle during the second subject's inclined walking. When the robot assisted in walking, compared to the 'no exo' walking where the second subject walked without exoskeleton robot, the hip joint flexed less, did not fully extend during the propulsion phase, and exhibited greater flexion in the swing phase. Reviewing the middle graph, which shows the direction of adduction/abduction, one can observe that the adduction angle is reduced during the initial weight-bearing stage due to the robot's assistance with the abduction moment compared to the 'no exo' condition. Like the flexion graph, the rate and magnitude of changes in the joint angles were not substantial. Analysis of the final rotation graph revealed that internal rotation surpassed 15 degrees throughout the entire walking phase with the robot's assistance.

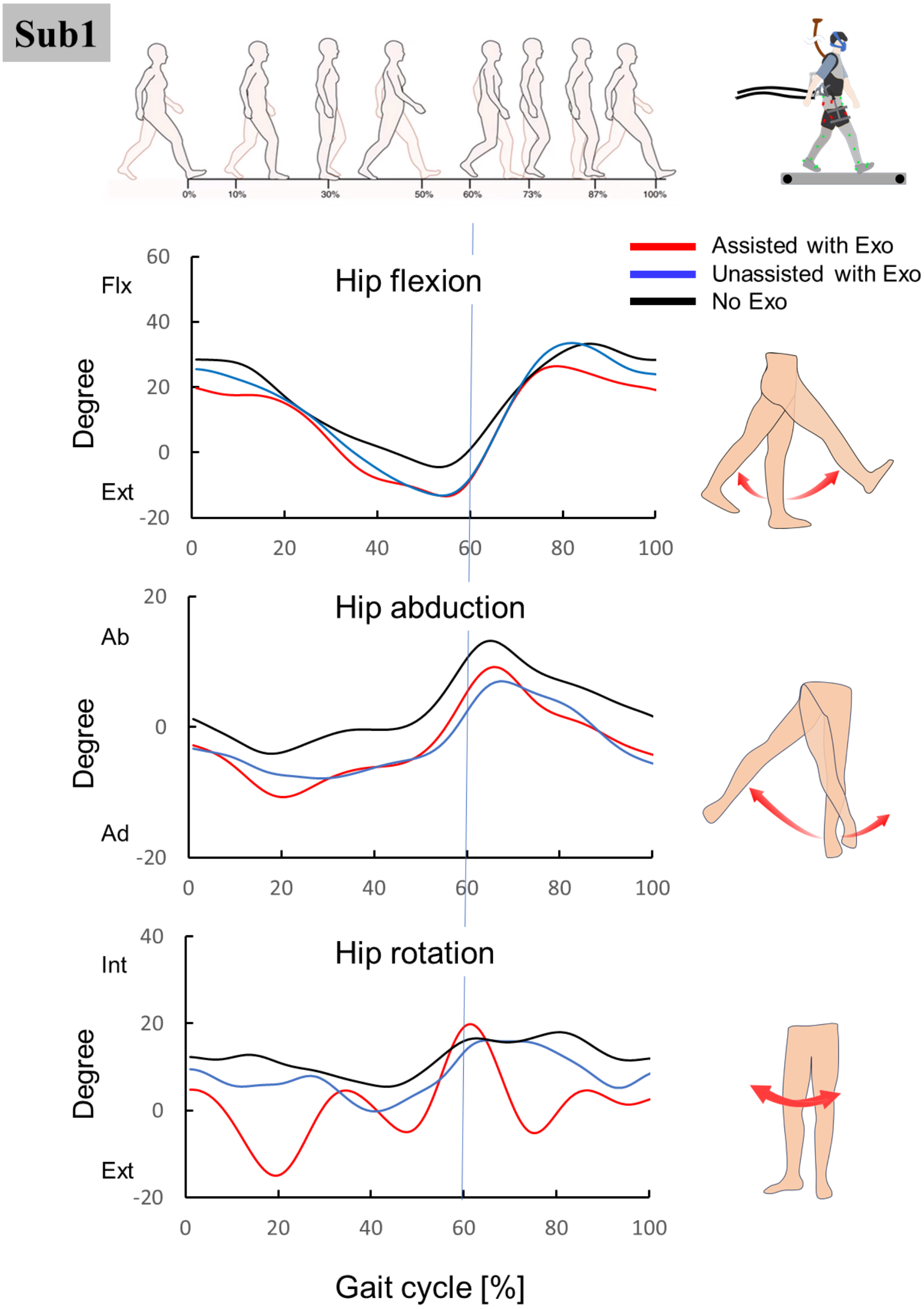

Fig. 3.3 Hip joint angle of Subject1. Walking on a treadmill with a level ground condition.

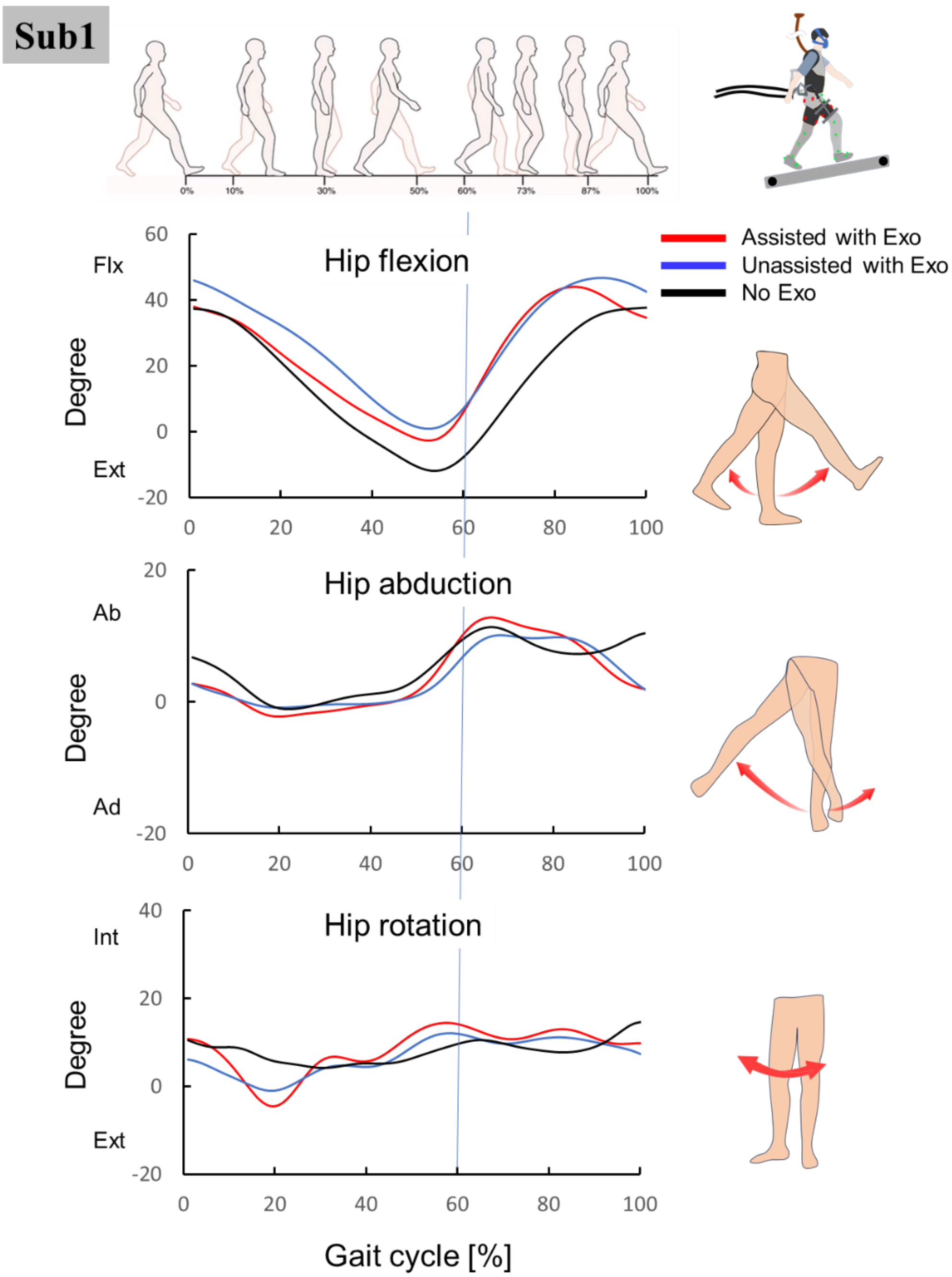

Fig. 3.4 Hip joint angle of Subject1. Walking on a treadmill with a 10% incline condition.

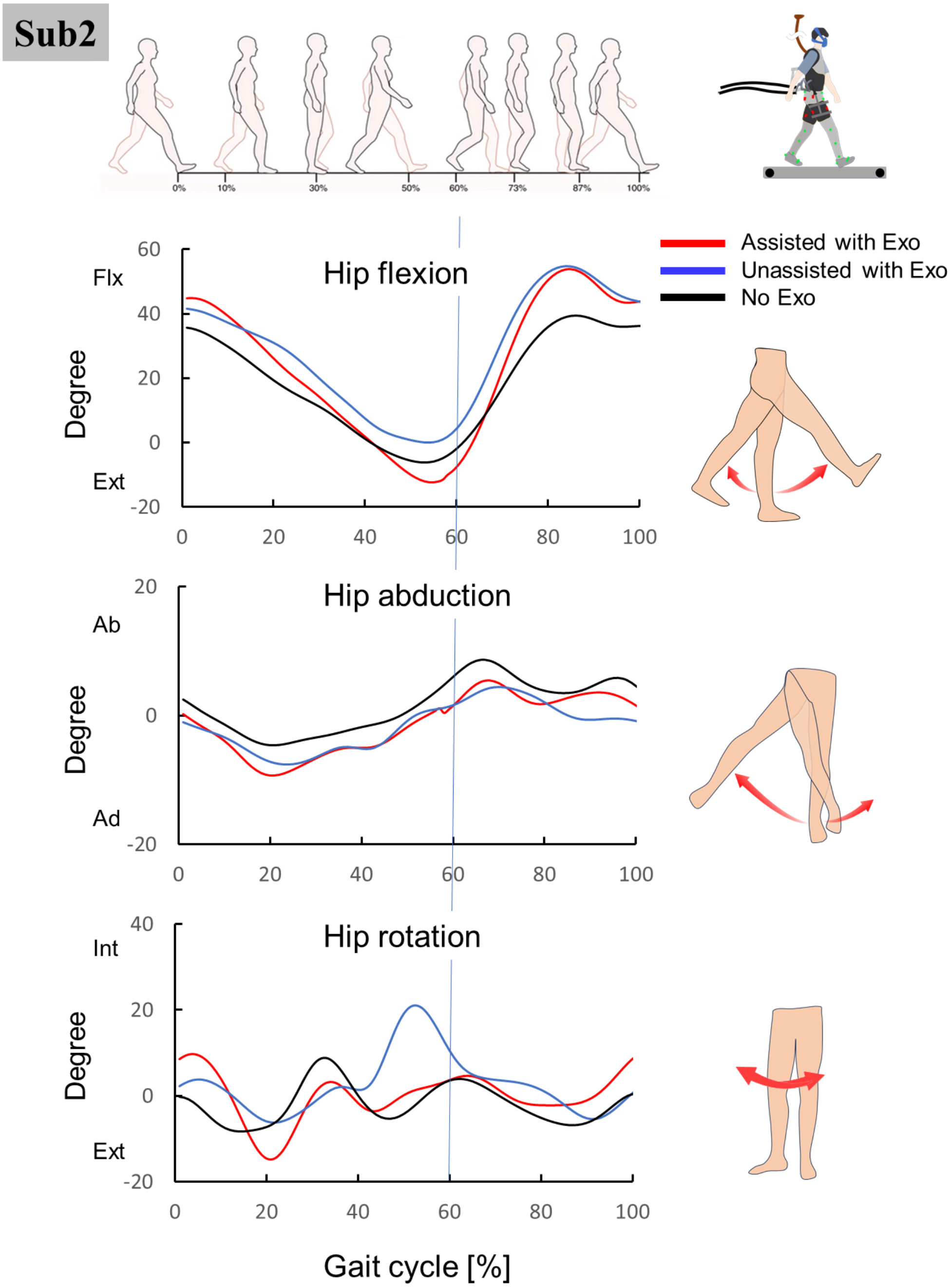

Fig. 3.5 Hip joint angle of Subject2. Walking on a treadmill with a level ground condition.

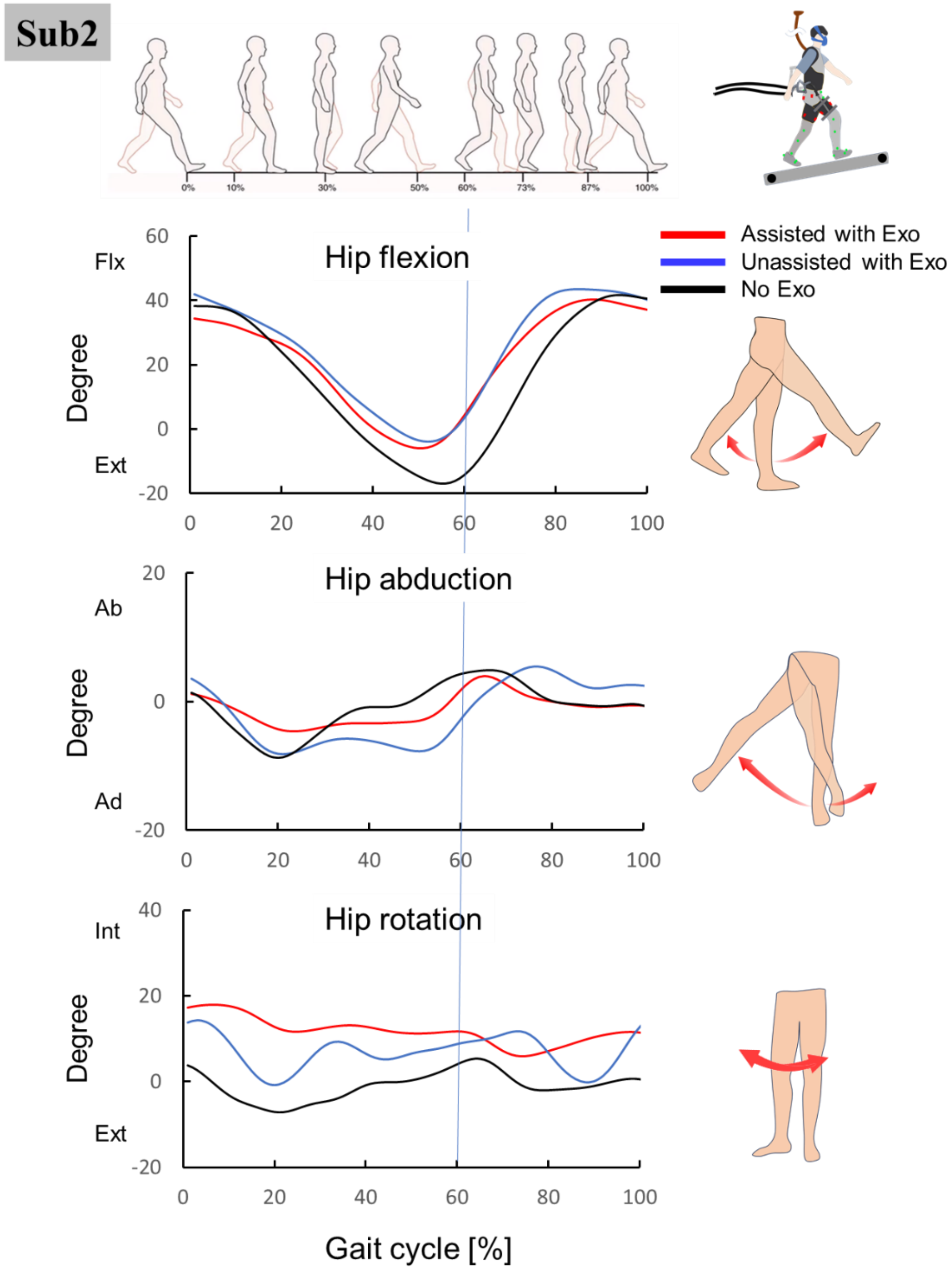

Fig. 3.6 Hip joint angle of Subject2. Walking on a treadmill with a 10% incline condition.

3.3 Kinetic analysis of hip joint center

One of the critical factors for verifying the clinical effectiveness of the R-4bar-R mechanism exoskeleton robot in this study is the output moment in the three directions of the hip joint. Based on computer simulation and preliminary test results before the clinical trial, we expect that the R-4bar-R mechanism robot's assistance with three-way moments will yield better results for walking on an incline than level ground. We conducted clinical tests on a split-belt treadmill equipped with a built-in ground reaction force device under two incline conditions (level ground and a 10% inclined slope) to verify this. We tested normal walking without the robot and assisted and unassisted conditions with the robot. The study results were averaged by extracting data from two consecutive strides during each five-minute walk for each walking condition. Subsequently, the obtained results were normalized by dividing them by the respective subject's body weight. The stride was recalibrated, with the reference point set from the right heel contact to the succeeding right heel contact, which was designated as 100%. We divided and plotted the moments for each subject in three directions (frontal, sagittal, and horizontal).

In the first flexion/extension moment graph of Fig. 3.7, the output moment in the body's flexion direction is higher when the robot assists condition compared to the 'no exo' condition, where the exoskeleton robot is not worn. Specifically, in the propulsion section corresponding to 30-40% of the gait phase, the difference is about three times as high, briefly dips at the beginning of the 50% swing, and then rises again. When walking only wearing the exoskeleton robot without assistance ('unassisted'), the overall tendency is similar to assisted walking but forms a lower output moment than when assisted. Examining the second abduction moment graph in Fig. 3.7, we can see that a high moment is formed when the robot assists throughout the entire walking cycle, and a high moment is output to the human body in both directions of abduction/adduction. Similar to the flexion moment pattern, a higher moment is formed during unassisted walking than in the 'no exo' condition, but a lower moment is formed during assisted walking. Looking at the last rotation moment graph in Fig. 3.7, unassisted and assisted walking demonstrate a pattern similar to 'no exo' walking, with a slightly higher moment output tendency in assisted walking only in the swing phase. Considering the causes of the difference in the first subject's hip joint flexion and abduction angle (Fig. 3.3), as well as the cause of the highest net metabolic rate (Fig. 3.1) in the assisted condition as inferred from the simulation results, a mismatch between the flexion moment required by the hip joint and the extension moment generated by the exoskeleton robot during 10-45% gait cycle causes increase of the moment when the human body tries to move forward against the exoskeleton robot's external force. Although the exoskeleton robot's abduction auxiliary moment is applied to the human body, the mechanical alignment of the R-4bar-R mechanism leans more towards adduction than the alignment of the human body's upright posture.

Consequently, the abduction stress is concentrated inside the hip joint. The reason for the excessive fluctuation of the rotation angle in Fig. 3.3 is that the robot's extension and abduction moment cause the thighs to rotate, as the external force of the robot is transmitted to the friction between the fastening tights worn for the robot and the human body. The excessive fluctuation of the rotation angle in Fig. 3.3 is likely due to the robot's external force being transmitted to the tights, worn for fastening the robot, resulting in the rotation of the tights from the resultant moment created by the robot's extension and abduction moments.

Looking at Fig. 3.8, which represents the output moment for the first subject's inclined walking, the hip joint moment appears in the following order of magnitude: assisted, unassisted, and 'no exo' conditions across the three graphs for flexion, abduction, and rotation moment. Excluding the rotation moment, it is lower than level walking, though the difference is not substantial. Moreover, in all three-moment graphs, there is no significant difference in the swing phase after 50% in the three conditions, and the flexion moment in the range of 50 to 70% temporarily shows the lowest moment in the assisted condition. The causes of improvement in the hip joint angle (Fig. 3.4) and the net metabolic rate, compared to the level walking condition inferred from the simulation results, seem to be twofold. First, the extension moment required by the human body until the loading response, which is about 35% of the section after heel contact, is appropriately provided. Secondly, after 50% of the swing phase, no interfering input moment against the flexion moment required by the human body has occurred. However, at the beginning of walking, an internal rotation moment, opposite to the external rotation moment required by the human body, was applied, resulting in a higher external rotation moment than unassisted walking. Furthermore, similar to level walking, the mechanical alignment of the R-4bar-R mechanism is more adducted than the alignment of the human body's upright posture, resulting in increased abduction stress inside the human hip joint and a subsequent increase in the abduction moment.

Figure 3.9 shows the change in the hip joint moment during the second subject's level ground walking. In the first flexion/extension moment graph, the output moment was lower in both unassisted and assisted conditions than in the 'no exo' condition during the initial 0-30% of the gait loading response. After this phase, the flexion moment was highest in the assisted condition. The second graph, depicting hip joint abduction, showed the highest moment overall in the assisted condition, and there was no significant difference between the three conditions after the 70% section, corresponding to the middle swing phase. In the third graph, showing the rotation moment, there was no significant difference between the unassisted and assisted conditions, but a difference in the external rotation direction compared to the 'no exo' condition was confirmed. The reason why the magnitude of the output moment in the abduction direction was the highest is likely because, similar to the first subject, the mechanical alignment of the R-4bar-R mechanism is more adducted than the alignment of the human body's upright posture, leading to a concentration of the abduction stress inside the hip joint. While it's unclear why the net metabolic rate in the assisted condition was exceptionally high for level ground walking compared to the first subject, this could be attributed to the difference in abduction and rotation moments and accumulated fatigue from consecutive testing. Looking at the hip joint moment results during the second subject's inclined walking in Fig. 3.10, similar to level walking, the moment results of both the unassisted and assisted conditions maintain higher values than the 'no exo' condition, displaying a similar pattern. After 60% of the walking phase or during the swing phase, there are no significant differences among the three conditions in terms of the three-direction moments. Although there is a difference in the size of the moment between the 'no exo' condition and both the unassisted and assisted conditions, the overall shape of the moment is similar. This result suggests that the lower pure metabolic rate compared to that of the first subject could be due to the mechanical arrangement of the R-4bar-R mechanism being a better match for the second subject.

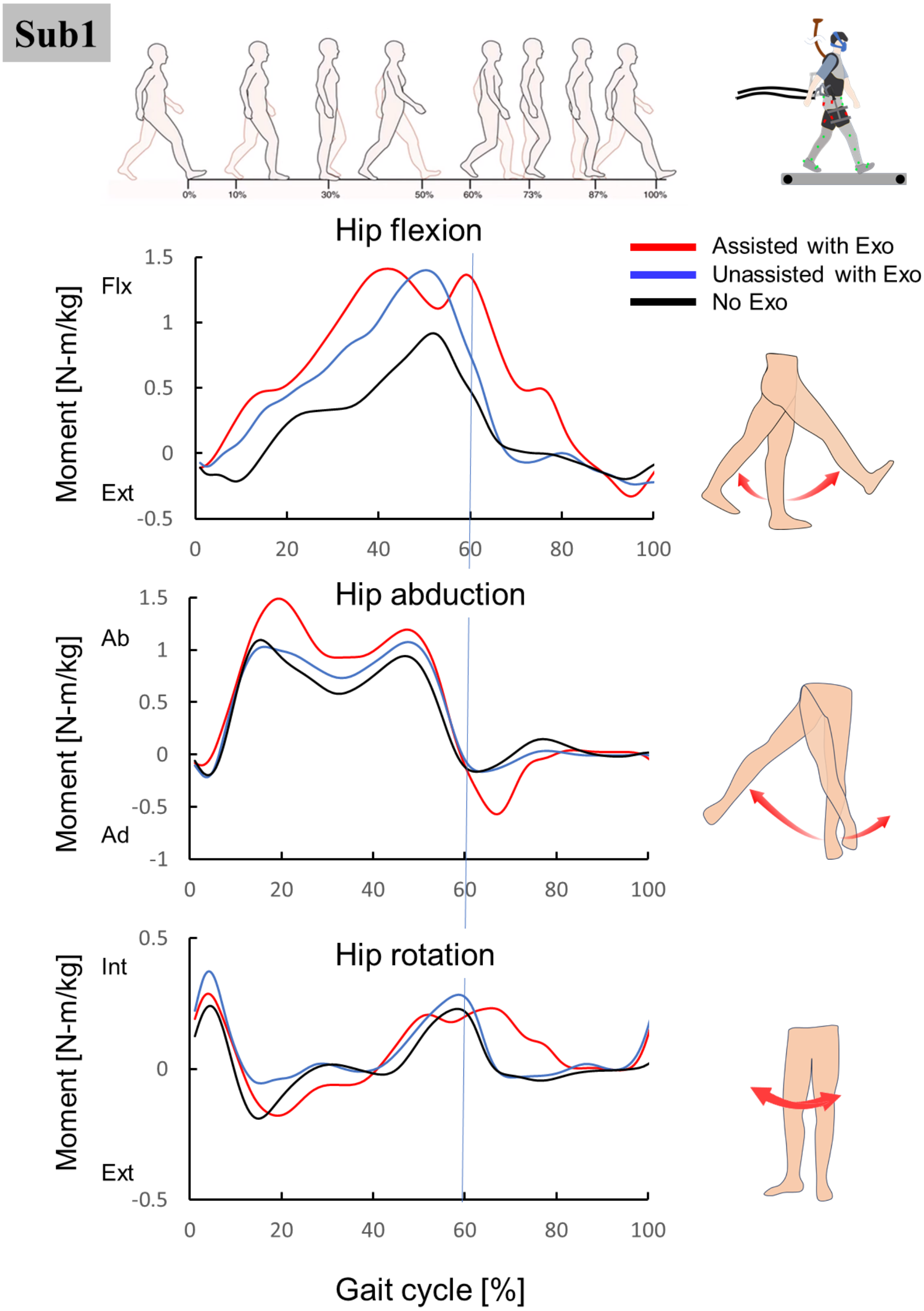

Fig. 3.7 Hip joint moment of Subject1. Walking on a treadmill with a level ground condition.

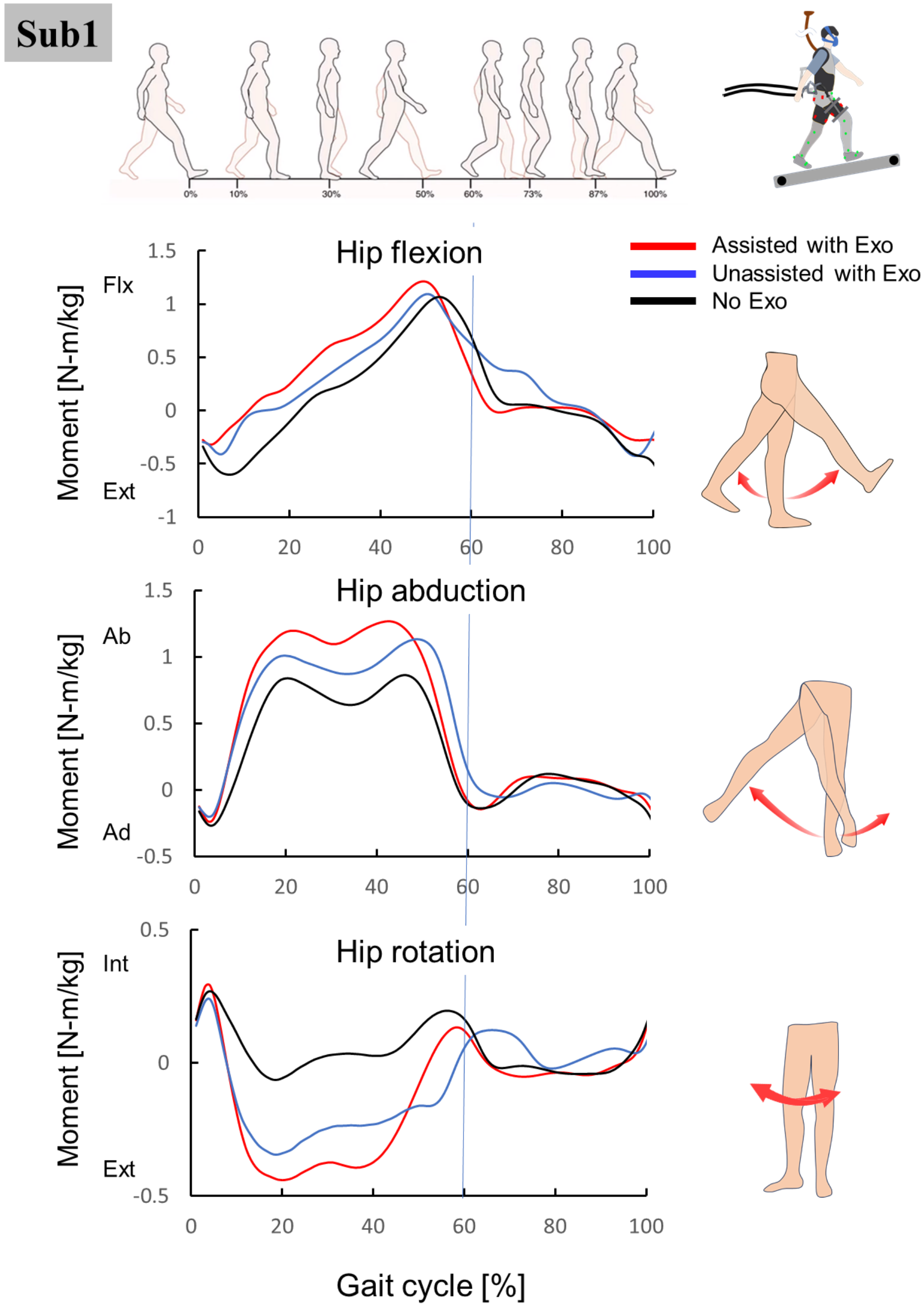

Fig. 3.8 Hip joint angle of Subject1. Walking on a treadmill with a 10% incline condition.

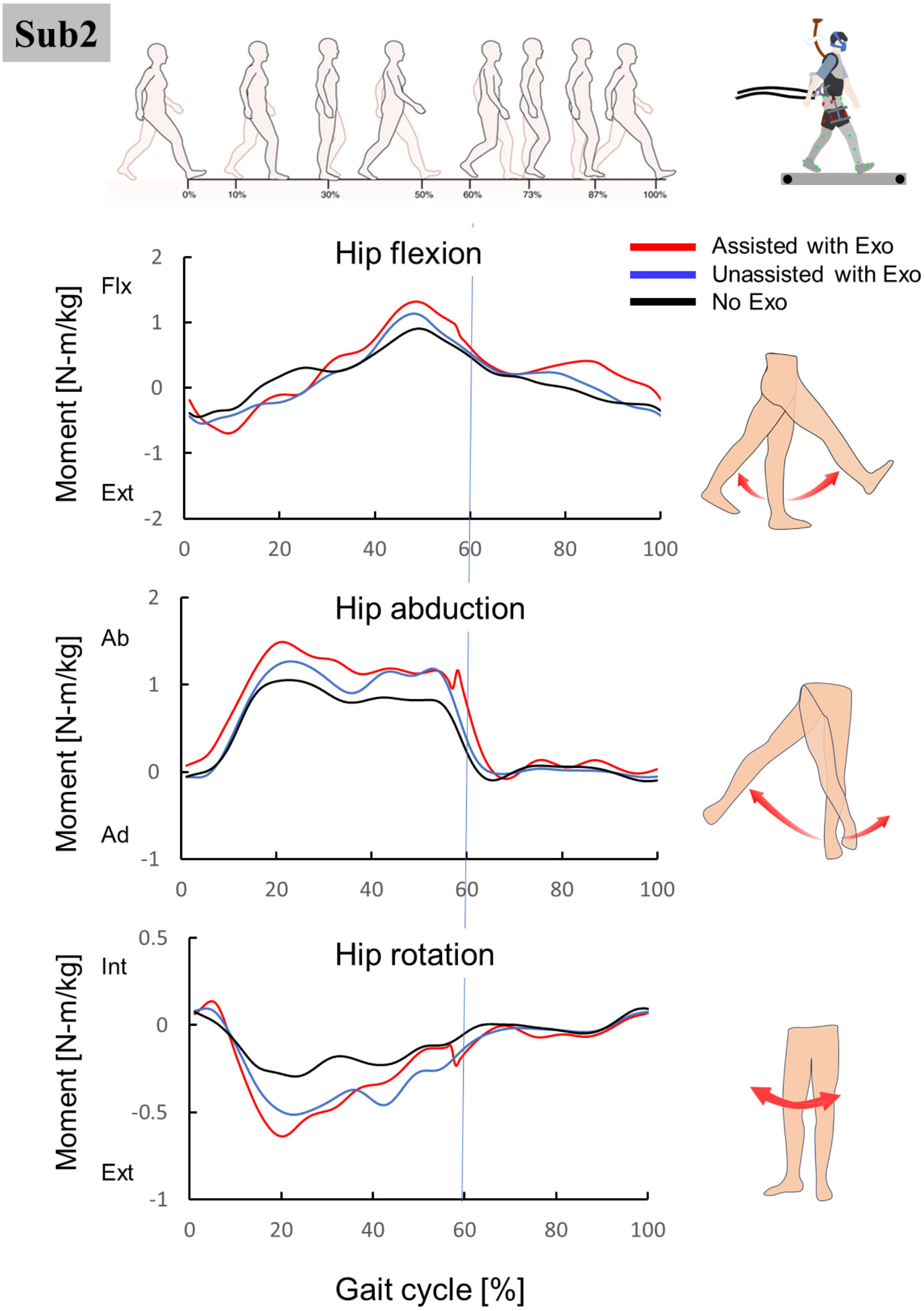

Fig. 3.9 Hip joint moment of Subject2. Walking on a treadmill with a level ground condition.

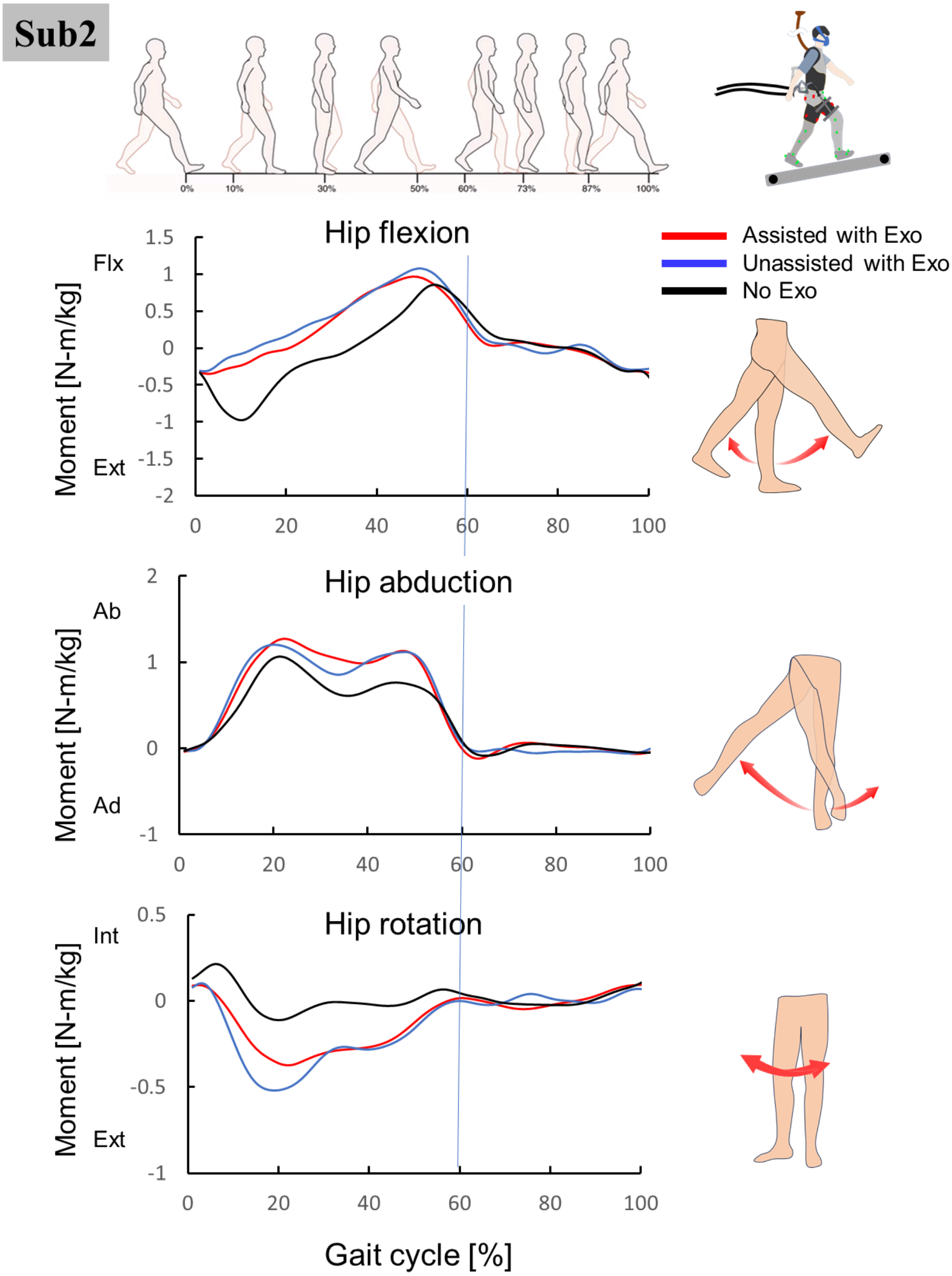

Fig. 3.10 Hip joint moment of Subject2. Walking on a treadmill with a 10% incline condition.

3.4 Questionnaire

Table 3.1 presents the survey results conducted on two participants following a clinical trial. The questionnaire used in this study is cited from the research by Gabi Zeilig et al. [33], which surveyed spinal cord injury patients about their perceived safety and fatigue after wearing an exoskeleton robot in a clinical trial. Table 3.1 utilized a 5-point Likert scale, ranging from "1 point, very much agree" to "5 points, very much disagree," the displayed score is the average of the two participants' responses. According to this survey, the participants responded neutrally concerning the ease of donning the exoskeleton robot, the difficulty in adapting to the external force imparted to their bodies by the robot after wearing it, and the robot's effectiveness in assisting with walking on level ground. They reported experiencing some discomfort and pain while using the robot and found breathing slightly challenging even after sufficiently adapting to wearing the robot during the clinical trial. Furthermore, they felt the robot was more beneficial while walking on slopes than on level ground. Lastly, they strongly agreed that the robot was safe.

Table 3.1 Satisfaction Questionnaire

	Statement	Likert scale AV
1	It was not difficult to adapt to the exoskeleton robot	3
2	Wearing/adjusting the exoskeleton is relatively simple	3
3	It was comfortable to exercise with the exoskeleton	4
4	The usage of the exoskeleton did not cause considerable pain	3.5
5	Walking with an exoskeleton has become more comfortable	3.5
6	I did not have breathing difficulties while training with the device	3.5
7	I felt that my gait improved when I got help from the robot on level walking	3
8	I felt that my gait improved when I got help from the robot on the incline	2
9	After completing the training, I felt safe using the exoskeleton	1.5

AV, average

CHAPTER 4.
Discussion

We designed an exoskeleton robot with an R-4bar-R mechanism, which assists simultaneously in three directions (flexion, abduction, and rotation), using the abduction moment generated in the human body during walking as the target moment. This robot was then applied to two healthy subjects to analyze the biomechanical results. Before the main clinical trial, we hypothesized through simulations using open-source data and several pilot tests that the R-4bar-R mechanism exoskeleton robot would be more beneficial for inclined walking than level ground walking, and to verify this, we analyzed pure metabolic, hip joint kinematics, and kinetic results. Contrary to the designer's intention, the net metabolic rate and three-way hip joint moment were predominantly high under assisted conditions for both level and inclined walking. This result contradicted previous studies that highlighted the significant metabolic reduction effects of the hip abduction device [6]. The causes for these unexpected results were analyzed based on the biomechanical results.

The first reason is that the R-4bar-R mechanism aligns with the end effector in the adduction direction, causing abduction stress to be consistently concentrated within the human hip joint. Consequently, even when the robot assists with the abduction moment, it fails to provide sufficient abduction displacement and moment necessary for walking. An improvement could be redesigning the mechanism to parallelize the misalignment between the mechanism and the thigh. The second reason is the inconsistent moment direction of the flexion and rotation moments that occur incidentally when the moment and abduction moment is set as the target torque in the human body. As this is a characteristic of the R-4bar-R mechanism when the abduction moment is set as the target moment, it will be necessary to refine the walking assistance strategy by setting the target moment that best aligns with the three directional moments required by the human body during walking. Thirdly, the significant moment generated in both unassisted and assisted conditions, as compared to the condition without the exoskeleton, can be attributed to the excessive weight of the R-4bar-R mechanism vest, which is approximately 9.8 kg. To reduce the weight of this mechanism, it would be necessary to improve the design or change the material of the mechanical part connecting the flexible shaft and the vest. The weight of the flexible shaft also needs to be offset by using an additional suspension device. Lastly, the auxiliary input moment used in this study may not be sufficient to assist walking. As referred to in previous studies, it would be necessary to recalculate and apply the desired torque, such as human-in-the-loop optimization [10]. In addition to these issues, other causes have been identified, like the method of integrating the robot and the human body. However, it will be necessary to analyze the kinematic and kinetic data of the hip joint through additional pilot tests after implementing the four significant improvements mentioned above.

CHAPTER 5.
Conclusion

Based on clinical trials, this study assesses the contribution of a spherical R-4bar-R mechanism exoskeleton robot to human walking and suggests directions for improvement using acquired biomechanical data. Before conducting a clinical trial with two subjects, simulations were performed using open-source data and pilot test results. This result led us to hypothesize that the R-4bar-R mechanism robot would have an advantage in inclined walking compared to level ground walking, a theory we subsequently validated through the clinical trial. In the main clinical trial, an infrared reflective marker system, a ground reaction force meter, and a breathing gas meter were used, and based on the results, the subject's kinematic, kinetic, and metabolic rates were analyzed. As expected, the clinical trial results showed slightly better biomechanical outcomes for inclined walking than level walking. However, when the alignment state between the R-4bar-R mechanism and the thigh and the desired abduction moment is determined, the moment in the other two directions (flexion, rotation) is subordinated to the determined characteristics, and it was concluded that it does not help normal walking. While the hip joint angle and moment yielded the most favorable results in the no exoskeleton condition, further research is required to understand why the net metabolic rate peaks during incline walking. One plausible explanation could be that subjects accumulated fatigue from wearing a respiratory gas mask (Cosmed, K5) for extended periods. In future studies, it is necessary to calculate the average value by conducting normal gait assessments before and after the test to enhance the reliability of the control group. The proposed modifications to this study's R-4bar-R mechanism design and control should be sufficiently validated for their impact on improving kinematic and kinetic data. Subsequently, recruiting more than 12 subjects and performing a biomechanical analysis could enhance research efficiency and yield significant results pertinent to the study of multi-axis hip joint assisted exoskeleton robots.

REFERENCES

[1] Collins SH, Bruce Wiggin M, Sawicki GS. Reducing the energy cost of human walking using an unpowered exoskeleton. Nature 2015;522:212–5. https://doi.org/10.1038/nature14288.

[2] Nuckols RW, Lee S, Swaminathan K, Orzel D, Howe RD, Walsh CJ. Individualization of exosuit assistance based on measured muscle dynamics during versatile walking. Sci Robot 2021;6. https://doi.org/10.1126/scirobotics.abj1362.

[3] MacLean MK, Ferris DP. Energetics of walking with a robotic knee exoskeleton. J Appl Biomech 2019;35:320–6. https://doi.org/10.1123/jab.2018-0384.

[4] Rodríguez-Fernández A, Lobo-Prat J, Font-Llagunes JM. Systematic review on wearable lower-limb exoskeletons for gait training in neuromuscular impairments. J Neuroeng Rehabil 2021;18. https://doi.org/10.1186/s12984-021-00815-5.

[5] Tan K, Koyama S, Sakurai H, Teranishi T, Kanada Y, Tanabe S. Wearable robotic exoskeleton for gait reconstruction in patients with spinal cord injury: A literature review. J Orthop Transl 2021;28:55–64. https://doi.org/10.1016/j.jot.2021.01.001.

[6] Dembia CL, Silder A, Uchida TK, Hicks JL, Delp SL. Simulating ideal assistive devices to reduce the metabolic cost of walking with heavy loads. PLoS One 2017;12. https://doi.org/10.1371/journal.pone.0180320.

[7] Bryan GM, Franks PW, Klein SC, Peuchen RJ, Collins SH. A hip–knee–ankle exoskeleton emulator for studying gait assistance. Int J Rob Res 2021;40:722–46. https://doi.org/10.1177/0278364920961452.

[8] Lenzi T, Carrozza MC, Agrawal SK. Powered hip exoskeletons can reduce the user's hip and ankle muscle activations during walking. IEEE Trans

Neural Syst Rehabil Eng 2013;21:938–48. https://doi.org/10.1109/TNSRE.2013.2248749.

[9] Malcolm P, Galle S, Derave W, de Clercq D. Bi-articular knee-ankle-foot exoskeleton produces higher metabolic cost reduction than weight-matched mono-articular exoskeleton. Front Neurosci 2018;12:1–14. https://doi.org/10.3389/fnins.2018.00069.

[10] Franks PW, Bryan GM, Martin RM, Reyes R, Lakmazaheri AC, Collins SH. Comparing optimized exoskeleton assistance of the hip, knee, and ankle in single and multi-joint configurations. Wearable Technol 2021;2. https://doi.org/10.1017/wtc.2021.14.

[11] Mooney LM, Rouse EJ, Herr HM. Autonomous exoskeleton reduces metabolic cost of human walking during load carriage. 2014.

[12] Haufe FL, Kober AM, Wolf P, Riener R, Xiloyannis M. Learning to walk with a wearable robot in 880 simple steps: a pilot study on motor adaptation. J Neuroeng Rehabil 2021;18. https://doi.org/10.1186/s12984-021-00946-9.

[13] Donelan JM, Kram R, Kuo AD. Mechanical and metabolic determinants of the preferred step width in human walking. Proc R Soc B Biol Sci 2001;268:1985–92. https://doi.org/10.1098/rspb.2001.1761.

[14] Sánchez N, Simha SN, Donelan JM, Finley JM. Using asymmetry to your advantage: Learning to acquire and accept external assistance during prolonged split-belt walking. J Neurophysiol 2021;125:344–57. https://doi.org/10.1152/jn.00416.2020.

[15] Bertram JEA, Ruina A. Multiple walking speed-frequency relations are predicted by constrained optimization. J Theor Biol 2001;209:445–53. https://doi.org/10.1006/jtbi.2001.2279.

[16] Ding Y, Kim M, Kuindersma S, Walsh CJ. Human-in-the-loop optimization of hip assistance with a soft exosuit during walking. Sci Robot 2018;3:1–9. https://doi.org/10.1126/scirobotics.aar5438.

[17] Seo K, Lee J, Park YJ. Autonomous hip exoskeleton saves metabolic cost of

walking uphill. IEEE Int Conf Rehabil Robot 2017:246–51. https://doi.org/10.1109/ICORR.2017.8009254.

[18] Galle S, Malcolm P, Derave W, De Clercq D. Adaptation to walking with an exoskeleton that assists ankle extension. Gait Posture 2013;38:495–9. https://doi.org/10.1016/j.gaitpost.2013.01.029.

[19] Galle S, Malcolm P, Collins SH, Clercq D De. Reducing the metabolic cost of walking with an ankle exoskeleton : interaction between actuation timing and power 2017:1–16. https://doi.org/10.1186/s12984-017-0235-0.

[20] Awad LN, Bae J, O'Donnell K, De Rossi SMM, Hendron K, Sloot LH, et al. A soft robotic exosuit improves walking in patients after stroke. Sci Transl Med 2017;9:1–13. https://doi.org/10.1126/scitranslmed.aai9084.

[21] [Robert Bogue 2018] Exoskeletons – a review of industrial applications.pdf n.d.

[22] Kim W, Lee H, Kim D, Han J, Han C. Mechanical design of the Hanyang Exoskeleton Assistive Robot(HEXAR). Int Conf Control Autom Syst 2014:479–84. https://doi.org/10.1109/ICCAS.2014.6988049.

[23] Garcia E, Arevalo JC, Mũnoz G, Gonzalez-de-Santos P. On the biomimetic design of agile-robot legs. Sensors 2011;11:11305–34. https://doi.org/10.3390/s111211305.

[24] Sangeux M, Pillet H, Skalli W. Which method of hip joint centre localisation should be used in gait analysis? Gait Posture 2014;40:20–5. https://doi.org/10.1016/j.gaitpost.2014.01.024.

[25] Besier TF, Sturnieks DL, Alderson JA, Lloyd DG. Repeatability of gait data using a functional hip joint centre and a mean helical knee axis. J Biomech 2003;36:1159–68. https://doi.org/10.1016/S0021-9290(03)00087-3.

[26] Stagni R, Leardini A, Cappozzo A, Grazia Benedetti M, Cappello A. Effects of hip joint centre mislocation on gait analysis results. J Biomech 2000;33:1479–87. https://doi.org/10.1016/S0021-9290(00)00093-2.

[27] Martelli D, Vashista V, Micera S, Agrawal SK. Direction-Dependent

Adaptation of Dynamic Gait Stability Following Waist-Pull Perturbations. IEEE Trans Neural Syst Rehabil Eng 2016;24:1304–13. https://doi.org/10.1109/TNSRE.2015.2500100.
[28] S.w.kang. Novel Topology Optimization Formulation for Wearable MotionForce Transmitting Robot Mechanisms Having General Joints n.d.
[29] Charalambous CP. Repeatability of kinematic, kinetic, and electromyographic data in normal adult gait. Class Pap Orthop 2014:399–401. https://doi.org/10.1007/978-1-4471-5451-8_101.
[30] Whittle MW. Clinical gait analysis: A review. Hum Mov Sci 1996;15:369–87. https://doi.org/10.1016/0167-9457(96)00006-1.
[31] Leboeuf F, Reay J, Jones R, Sangeux M. The effect on conventional gait model kinematics and kinetics of hip joint centre equations in adult healthy gait. J Biomech 2019;87:167–71. https://doi.org/10.1016/j.jbiomech.2019.02.010.
[32] Brockway JM. Derivation of formulae used to calculate energy expenditure in man. Hum Nutr Clin Nutr 1987;41:463–71.
[33] Zeilig G, Weingarden H, Zwecker M, Dudkiewicz I, Bloch A, Esquenazi A. Safety and tolerance of the ReWalk™ exoskeleton suit for ambulation by people with complete spinal cord injury: A pilot study. J Spinal Cord Med 2012;35:96–101. https://doi.org/10.1179/2045772312Y.0000000003.

ABSTRACT (KOREAN)

R-4bar-R 메커니즘 고관절 외골격 로봇의 생체역학적 평가

김 태 환
서울대학교 대학원
기계공학부

본 연구는 임상시험을 통해 구면 회전 조인트 – 4절 – 회전 조인트 메커니즘을 갖는 외골격 로봇이 인간의 보행에 미치는 기여도를 평가하고, 임상시험을 통해 취득한 생체역학적 정보를 활용하여 외골격 로봇의 개선 방향을 제시하는 연구이다. 본 연구에서 사용한 외골격 로봇은 엉덩 관절에 구면 회전 조인트 – 4절 – 회전 조인트 구조를 적용함으로써 한 개의 구동기로 세 방향(굴곡, 외전, 회전) 모두 보조하여, 시상면 보행 보조에 국한된 전통적인 외골격 로봇의 한계를 극복하였다. 본 임상시험 전 오픈 소스 자료를 이용한 모의 실험과 여러 차례 예비 임상시험을 통해 평지 보행 보다 경사 보행에 유리한 결과를 나타낼 것이라 가정하였고, 착용자 체중의 10%에 해당하는 외전 방향 목표 토크를 설정하였다. 이 가설을 검증하고 외골격 로봇의 생체역학적

평가를 위해 임상시험 절차를 설계하였고, 하지에 24개의 적외선 반사 마커를 부착하고 지면반력 측정기가 내장된 트레드밀에서 일정한 속도(1.25 m s^{-1})로 보행하며 임상시험을 수행하였다. 임상시험은 평지와 10% 기울기에서 각각 세 가지(로봇을 입지 않은 일반보행, 로봇을 입고 보조력을 받는 보행, 로봇을 입고 보조력을 받지 않은 보행) 보행 조건을 5분씩 수행하였으며, 두 명의 건강한 피험자를 모집하여 엉덩관절의 각도, 모멘트 호흡가스 결과를 취득하여 분석하였다. 시험 결과는 평지 보행과 경사 보행 모두 외골격 로봇의 도움을 받으며 보행할 때 신진대사율과 관절 모멘트가 대부분 높게 나타났다. 생체역학적 결과를 가지고 분석한 결과 메커니즘 설계의 의도와 다른 결과가 나타난 원인은 다양하였다. 첫 번째로 메커니즘과 착용자의 허벅지 정렬이 내전 방향으로 정렬되어 엉덩관절에 내전 응력이 집중되어 있기 때문에 충분한 외전 모멘트가 전달되지 않았고, 두 번째로 외골격 로봇이 엉덩관절로 전달한 굴곡, 회전 모멘트 방향이 보행시 필요한 모멘트의 방향과 일치하지 않는 보행 구간이 많았으며, 인체에 결합된 외골격 로봇의 무게와 동력전달을 위한 신축성 회전 축의 무게가 과도하기 때문이었다. 본 연구는 유효한 보조 효과를 얻기 위한 방법으로 첫 번째로 회전 조인트 – 4절 – 회전 조인트 메커니즘과 말단 효과장치인 허벅지의 정렬을 평행하게 맞추고, 두 번째로 목표

토크를 외전 방향 하나에 맞추지 않고 인체에서 필요한 세 방향 모멘트의 방향과 균일하게 일치하는 최적 제어 및 착용자 보행 학습을 통한 자동제어 모델을 적용하며, 세 번째로 로봇의 재료 변경 및 신축성 회전 축 연결 부위 설계 수정을 통한 경량화가 필요하다고 제안하였다. 이 연구에서 제언한 구면 회전 조인트 – 4절 – 회전 조인트 구조를 갖는 엉덩관절 보조 외골격 로봇의 유효성 및 개선 방안은 단일 관절을 갖는 외골격 로봇 연구의 한계를 극복하고 다축 관절 외골격 로봇 연구를 확장하는데 크게 기여할 수 있을 것으로 기대한다.

주요어: 생체역학, 운동역학, 신진대사, 외골격 로봇, 착용형 로봇, 보행분석

학 번: 2021-21839